JOURNAL OF SOLID STATE CHEMISTRY 64, 261–269 (1986)

Some Substitutional Chemistry in Known Ternary and Quaternary Chalcogenides

PHILIP J. SQUATTRITO, STEVEN A. SUNSHINE, AND JAMES A. IBERS

Department of Chemistry, Northwestern University, Evanston, Illinois 60201

Received December 8, 1985

New ternary and quaternary transition-metal chalcogenides have resulted from substitutional chemistry of known phases. $Ta_2Ni_3S_8$ and $Ta_2Pt_3Se_8$ have been synthesized and characterized by single-crystal X-ray techniques. These compounds adopt the $Nb_2Pd_3Se_8$ structural type. Hence in $Ta_2Ni_3S_8$ Ni occupies both square-planar and square-pyramidal sites as similarly does Pt in $Ta_2Pt_3Se_8$. The electrical conductivity of $Ta_2Ni_3S_8$ establishes its semiconducting behavior. Ta has been substituted for Nb in the $Nb_2Pd_{0.71}Se_5$ type to yield $Ta_2Pd_{0.89}S_5$ which has been characterized by single crystal X-ray techniques. The square-planar Pd sites in the van der Waals' gap of this layer structure are 78.6(4)% occupied. This compound shows metallic behavior. The compound $Co_2Nb_4PdSe_{12}$ has been synthesized and characterized by single-crystal X-ray techniques. It is of the $Co_2Ta_4PdSe_{12}$ structural type and thus contains Nb in both trigonal prismatic and octahedral sites.

Introduction

The structure of many solid-state inorganic compounds can be described in terms of cations filling interstices in a closest-packed anion array. An alternative description is in terms of the linking of metal-centered polyhedra. We find this alternative description useful as it enables us to use the geometrical preferences of various metal centers, as known from the coordination chemistry of molecular systems, in the design of new materials (*1–5*). We have previously described how some of these new structures in the Nb,Ta/Pd/S,Se systems can be thought of as arising from the linking of Nb- or Ta-centered trigonal prisms and Pd-centered square planes or square pyramids (*1, 3, 5*). The substitution of Ni for Pd has led to new structures (e.g., Ta_2NiQ_5, Q = S, Se (*4*)), since the stereochemical preferences of Ni are not limited to square-planar and square-pyramidal geometries (*6–8*). But can Ni or Pt, whose stereochemical preferences do not parallel exactly those of Pd, be substituted for Pd in some of these structures? Can Nb, which shows a strong preference for trigonal-prismatic coordination, be substituted for Ta in octahedral coordination (*2*) in another of these structures? In short, we seek to test experimentally some of the limits of this concept of stereochemical preference and we report our results here.

Experimental

Syntheses of $Ta_2Ni_3S_8$ and $Ta_2Pt_3Se_8$. A stoichiometric combination of the elements, Ta powder (AESAR 99.98%), Ni

0022-4596/86 $3.00

TABLE I

CRYSTAL DATA AND INTENSITY COLLECTION FOR NEW CHALCOGENIDES

	$Ta_2Ni_3S_8$	$Ta_2Pt_3Se_8$	$Ta_2Pd_{0.89}S_5$	$Co_2Nb_4PdSe_{12}$
Mol. Wt.	794.5	1578.8	616.89	1543.41
Space group	D^9_{2h}-*Pbam*	D^9_{2h}-*Pbam*	C^3_{2h}-*C2/m*	C^3_{2h}-*C2/m*
a, Å	14.092(4)	15.003(6)	12.204(7)	12.871(9)
b, Å	10.078(3)	10.687(6)	3.269(2)	3.402(2)
c, Å	3.314(1)	3.541(1)	15.183(8)	19.436(14)
β, deg.[a]			104.48(2)	110.87(3)
V, Å^3	471	568	587	795
Z	4	4	4	2
T of data collection, K	123[c]	123[c]	123[b]	123[c]
Crystal vol., mm^3	1.51×10^{-4}	1.16×10^{-5}	3.7×10^{-5}	5.3×10^{-5}
Crystal shape	Needle bound by {210}, ($\bar{1}$10) ($\bar{1}$20) {001}	Needle bound by ($\bar{2}$10) (1$\bar{1}$0) (3$\bar{1}$0) ($\bar{1}$10) (110) (1$\bar{2}$0) (120) (00$\bar{1}$) (001)	Flattened needle bound by {20$\bar{1}$}, {010}, (20$\bar{3}$), and ($\bar{1}$01)	Needle bound by {20$\bar{1}$}, {001}, and {010}
Radiation	Graphite monochromatized Mo$K\alpha$ ($\lambda(K\alpha_1)$ = 0.7093 Å)			
Linear abs. coeff., cm^{-1}	305	816	420	330
Transmission factors[d]	0.392–0.576	0.362–0.680	0.398–0.902	0.588–0.789
Detector aperture, mm	Horizontal—3.0 Vertical—3.0 17.3 cm from crystal	Horizontal—3.0 Vertical—3.0 17.3 cm from crystal	Horizontal—5.0 Vertical—5.0 32 cm from crystal	Horizontal—3.0 Vertical—2.25 17.3 cm from crystal
Takeoff angle, deg.	2.8	2.3	3.2	4.0
Scan speed, deg. min^{-1}	1.33[f] $0° < \theta \leq 25°$ 1.07 $25° < \theta \leq 35°$	1.60[f] $0° < \theta \leq 30°$ 1.33 $30° \leq \theta$ 32.5°	2.0[e]	2.0[f]
Scan type	$\theta - 2\theta$	$\theta - 2\theta$	$\theta - 2\theta$	ω
Scan range, deg.	0.9 below $K\alpha_1$ to 0.9 above $K\alpha_2$	1.0 below $K\alpha_1$ to 1.0 above $K\alpha_2$	1.1 below $K\alpha_1$ to 1.1 above $K\alpha_2$	−0.9 to +0.9 in ω
λ^{-1} sin θ, limits, Å^{-1}	0.0612–0.8062 $2.40 \leq \theta(\text{Mo}K\alpha_1) \leq 35°$	0.0659–0.7575 $2.70 \leq \theta(\text{Mo}K\alpha_1) \leq 32.5$	0.0492–0.7678 $2° \leq \theta(\text{Mo}K\alpha_1) \leq 33°$	0.0737–0.7049 $3° \leq \theta(\text{Mo}K\alpha_1) \leq 30°$
Background counts	¼ of scan range on each side of reflection		10 sec at each end of scan with rescan option[e]	¼ of scan range on each side of reflection
Data collected	$\pm h, \pm k, \pm l$	$+h, +k \pm l$ ($0° < \theta \leq 20°$) $+h, +k + l$ ($20° < \theta \leq 32.5°$)	$\pm h, \pm k, \pm l$	$\pm h, \pm k, \pm l$
p factor	0.04	0.04	0.04	0.04
No. unique data including $F_o^2 < 0$	1268	1182	1268	1341
No. unique data including $F_o^2 < 3\sigma(F_o^2)$	723	554	865	926
$R(F^2)$	0.093	0.123	0.074	0.103
$R_w(F^2)$	0.116	0.150	0.098	0.123
R (on *F* for $F_o^2 > 3\sigma(F_o^2)$)	0.049	0.067	0.041	0.051
Error in observation of unit wt. e^2	0.98	1.04	1.09	1.25

[a] All cell refinements constrained the appropriate angles to 90°.

[b] The low-temperature system for the Picker FACS-1 diffractometer is based on a design by Huffman, J. C., Ph.D. thesis, Indiana University, 1974.

[c] The low-temperature system for the Nonius CAD4 diffractometer is from a design by Professor J. J. Bonnet and S. Askenazy and is commercially available from Soterem, Z. T. de Vic, 31320 Castanet-Tolosan, France.

[d] The analytical method as employed in the Northwestern absorption program, AGNOST, was used for the absorption correction (J. de Meulenaer and H. Tompa, *Acta Crystallogr.* **19**, 1014 (1965)).

[e] The Picker FACS-1 diffractometer was operated under the Vanderbilt disk oriented system (P. G. Lenhert, *J. Appl. Crystallogr.* **8**, 568 (1975)).

[f] Reflections with $\sigma(I)/I > 0.33$ were rescanned up to a maximum time of 3 min.

powder (ALFA 99.9%) or Pt powder (AESAR 99.98%), and S powder (ATOMERGIC 99.999%) or Se powder (ATOMERGIC 99.999%) were combined in a silica tube that was then evacuated (~10^{-5} Torr). For $Ta_2Ni_3S_8$ bromine (~2 mg/cm^3 of tube volume) was condensed into the reaction tube. The vessel was sealed and placed in a furnace and heated at 1000 K for 288 hr (Ni compound) or at 1273 K for 250 hr (Pt compound). After this time the furnace was radiatively cooled. Long gray-black fibrous

needles up to 1 cm in length were dispersed throughout the tube containing the Ni charge, whereas small gray crystals in the form of flat needles generally less than 0.1 mm in length grew in the tube with the Pt charge. For each the presence of the three elements was confirmed with the electron microprobe of an EDAX-equipped Cambridge S-4 scanning electron microscope.

Synthesis of $Ta_2Pd_{0.89}S_5$. In addition to the sources noted above, Pd powder (AESAR 99.95%) was used. The initial synthesis of the compound $Ta_2Pd_{0.89}S_5$ was accomplished by heating a 1 : 3 : 4 (Ta : Pd : S) ratio of the elements, along with ~3 μl of Br_2, in a sealed, evacuated silica tube for 7 days at 1000 K. This reaction yielded many small shiny black needle-shaped crystals up to 2 mm in length. Analysis with an electron microprobe confirmed the ternary nature of these crystals and an approximate composition of 2 : 1 : 5 (Ta : Pd : S). Subsequently, this compound was obtained in nearly pure powder form by direct combination of a 2 : 1 : 5 ratio of the elements heated for 4 weeks at 1000–1100 K with several intermittent grindings. The X-ray powder diffraction pattern for this sample, obtained with Ni-filtered Cu$K\alpha$ radiation on a Rigaku Geigerflex powder diffractometer, was in satisfactory agreement with that generated from the known structure (*2*) of $Nb_2Pd_{0.71}Se_5$ by substitution of Ta for Nb and S for Se. Crystal growth from such powders is sluggish, even for samples heated at 1100 K in the presence of Br_2 over a period of weeks. In general the best crystals are obtained by direct combination with the use of a substantial excess of Pd (e.g., a 1 : 3 : 4 ratio) with Br_2 at 1100–1125 K.

Synthesis of $Co_2Nb_4PdSe_{12}$. In addition to the sources noted above, Co powder (ALFA 99.8%) was used. Synthesis was initiated by heating a stoichiometric ratio of the elements for 3 days at 725 K in a sealed, evacuated silica tube, after which the sample was crushed and loaded into a fresh tube. The charge was then heated for 24 hr at 825 K and 7 days at 1125 K. A powdery mass covered with many small needle crystals was obtained. A qualitative electron microprobe analysis confirmed that all four elements were present in the crystals.

Crystallographic studies. Preliminary Weissenberg photography on the four compounds established unit cells later confirmed by diffractometry. Collection of intensity data, solution of the structures, and refinement were carried out by methods standard in this laboratory (*1–5*). Final refinements were on F_o^2 and involved anisotropic thermal parameters. Details are summarized in Table I. For $Ta_2Pd_{0.89}S_5$ the approximate composition was established from initial refinements of the intensity data. The data were then corrected for absorption with the use of a linear absorption coefficient calculated for this composition. From the final refinement cycle the composition of the crystal used is $Ta_2Pd_{0.839(2)}S_5$. The other three compounds were assumed to be stoichiometric. The reasonableness of the anisotropic thermal parameters for the various atoms in these structures suggests that any deviations from stoichiometric composition are very small.

Residual difference electron densities in these four structures are all around 2–3% of the height of the heaviest element in a given structure. Analysis of $\Sigma w(F_o^2 - F_c^2)^2$ as a function of setting angles and Miller indices for each of these structures reveals no unusual trends.

Table II presents the positional parameters and equivalent isotropic thermal parameters for the four compounds. Tables III[1] and IV[1] present listings of structure am-

[1] See NAPS document No. 04387 for 30 pages of supplementary material. Order from NAPS, c/o Microfiche Publications, P.O. Box 3513, Grand Central Station, New York, NY 10163. Remit in advance in U.S. funds only $4.00 for microfiche copy or $10.75 for photocopy. Foreign orders add $4.50 for postage and handling, for the first 20 pages, and $1.00 for additional 10 pages of material. Remit of $1.50 for postage of any microfiche orders.

TABLE II

FINAL PARAMETERS AND EQUIVALENT ISOTROPIC THERMAL PARAMETERS

Atom	Wyckoff notation	Site symmetry	x	y	z	B_{eq} (Å^2)
			$Ta_2Ni_3S_8$			
Ta	4g	m	0.119005(45)	0.203894(64)	½	0.27(1)
Ni(1)	2a	2/m	0	0	0	0.42(6)
Ni(2)	4g	m	0.22461(15)	0.37118(21)	0	0.40(4)
S(1)	4g	m	0.99122(27)	0.22059(40)	0	0.39(7)
S(2)	4g	m	0.15540(27)	0.02894(41)	0	0.39(7)
S(3)	4g	m	0.28684(27)	0.24675(39)	½	0.35(7)
S(4)	4h	m	0.12952(29)	0.44275(38)	½	0.43(7)
			$Ta_2Pt_3Se_8$			
Ta	4g	m	0.11973(11)	0.21332(17)	½	0.45(4)
Pt(1)	2a	2/m	0	0	0	0.54(5)
Pt(2)	4g	m	0.21778(11)	0.37395(16)	0	0.38(3)
Se(1)	4g	m	0.99162(30)	0.22842(45)	0	0.6(1)
Se(2)	4g	m	0.15818(27)	0.04147(41)	0	0.47(8)
Se(3)	4g	m	0.28908(28)	0.24854(41)	½	0.56(9)
Se(4)	4g	m	0.11804(28)	0.45328(42)	½	0.58(9)
			$Ta_2Pd_{0.89}S_5$			
Ta(1)	4i	m	0.075093(50)	½	0.182425(41)	0.26(1)
Ta(2)	4i	m	0.151169(50)	0	0.376921(40)	0.22(1)
Pd(1)	2a	2/m	0	0	0	0.33(3)
Pd(2)[a]	2c	2/m	0	0	½	0.33(4)
S(1)	4i	m	0.35171(32)	0	0.49455(25)	0.32(7)
S(2)	4i	m	0.25134(32)	½	0.30386(26)	0.40(7)
S(3)	4i	m	0.17395(32)	0	0.10883(26)	0.41(7)
S(4)	4i	m	0.42399(32)	½	0.12598(25)	0.35(7)
S(5)	4i	m	0.49872(32)	0	0.31617(25)	0.33(7)
			$Co_2Nb_4PdSe_{12}$			
Pd	2a	2/m	0	0	0	0.48(4)
Nb(1)	4i	m	0.52803(12)	0	0.149074(81)	0.43(3)
Nb(2)	4i	m	0.66431(12)	0	0.406732(80)	0.43(3)
Se(1)	4i	m	0.65590(13)	½	0.116682(91)	0.39(4)
Se(2)	4i	m	0.48991(13)	½	0.609313(94)	0.49(4)
Se(3)	4i	m	0.82711(13)	½	0.453107(90)	0.36(4)
Se(4)	4i	m	0.41639(13)	0	0.232661(93)	0.53(4)
Se(5)	4i	m	0.37884(13)	½	0.072614(91)	0.45(4)
Se(6)	4i	m	0.68584(13)	0	0.280668(90)	0.46(4)
Co	4i	m	0.55212(16)	½	0.28070(11)	0.29(5)

[a] Occupancy = 0.786(4).

plitudes and anisotropic thermal parameters, respectively, for these compounds.

Electrical conductivity measurements. Four-probe single-crystal conductivity measurements were made for $Ta_2Ni_3S_8$ along the needle axis c and for $Ta_2Pd_{0.89}S_5$ along the needle axis b following established procedures (*9*). Conductivity mea-

TABLE V

SELECTED BOND DISTANCES (Å) AND ANGLES (DEG.) FOR $Ta_2Ni_3S_8$ AND $Ta_2Pt_3Se_8$

$Ta_2Ni_3S_8$		$Ta_2Pt_3Se_8$	
Ta–2S(1)	2.453(3)	Ta–2Se(1)	2.618(4)
Ta–2S(2)	2.474(3)	Ta–2Se(2)	2.616(4)
Ta–1S(3)	2.404(4)	Ta–1Se(3)	2.569(5)
Ta–1S(4)	2.412(4)	Ta–1Se(4)	2.565(5)
Ta–2Ni(2)	2.793(2)	Ta–2Pt(2)	2.872(2)
Ta–2Ni(1)	3.127(1)	Ta–2Pt(1)	3.400(2)
Ta–2Ta	3.314(1)	Ta–2Ta	3.541(1)
Ni(1)–2S(1)	2.227(4)	Pt(1)–2Se(1)	2.445(5)
Ni(1)–2S(2)	2.209(4)	Pt(1)–2Se(2)	2.414(4)
Ni(1)–2Ni(1)	3.314(1)	Pt(1)–2Pt(1)	3.541(1)
Ni(2)–2S(3)	2.256(3)	Pt(2)–2Se(3)	2.465(3)
Ni(2)–2S(4)	2.250(3)	Pt(2)–2Se(4)	2.469(3)
Ni(2)–1S(2)	2.321(5)	Pt(2)–1Se(2)	2.582(5)
Ni(2)–2Ni(2)	3.314(1)	Pt(2)–2Pt(2)	3.541(1)
S(1)–Ta–S(1)	85.0(1)	Se(1)–Ta–Se(1)	85.1(1)
S(1)–Ta–S(2)	75.4(1)	Se(1)–Ta–Se(2)	75.4(1)
S(1)–Ta–S(4)	88.7(1)	Se(1)–Ta–Se(4)	86.0(1)
S(3)–Ta–S(4)	76.1(1)	Se(3)–Ta–Se(4)	82.1(1)
S(1)–Ni(1)–S(2)	85.6(1)	Se(1)–Pt(1)–Se(2)	82.4(1)
S(2)–Ni(2)–S(3)	95.6(1)	Se(2)–Pt(2)–Se(3)	93.7(1)
S(3)–Ni(2)–S(3)	94.6(1)	Se(3)–Pt(2)–Se(3)	91.8(2)
S(3)–Ni(2)–S(4)	82.4(1)	Se(3)–Pt(2)–Se(4)	86.2(1)

surements were not made for $Ta_2Pt_3Se_8$ or for $Co_2Nb_4PdSe_{12}$ because suitable crystals were not available.

Results

$Ta_2Ni_3S_8$ and $Ta_2Pt_3Se_8$. Selected bond distances and angles for the compounds $Ta_2Ni_3S_8$ and $Ta_2Pt_3Se_8$ are given in Table V. A drawing of the structure is presented in Fig. 1. These compounds and $Nb_2Pd_3Se_8$ (*1*) and $Ta_2Pd_3Se_8$ (*2*) form an isostructural set. This structural type has previously been described in detail (*1*). The metrical details for $Ta_2Pt_3Se_8$ are similar to those of $Ta_2Pd_3Se_8$ as the crystal radii for Pd and Pt are similar (*10*). Bond distances for $Ta_2Ni_3S_8$ are consistent with those found in Ta_2NiS_5 (*4*). In general the bond distances and angles in $Ta_2Ni_3S_8$ follow the same trends as those in $Ta_2Pd_3Se_8$. For example, the basal distances ($M(2)$–$Q(3)$, $M(2)$–$Q(4)$, M = Ni or Pt, Q = S or Se) of the square pyramid are somewhat shorter than the apical distance ($M(2)$–$Q(2)$). In each of the present structures the $M(2)$ atom lies above the basal plane of the square pyramid and this results in a $Q(3)$–$M(2)$–$Q(4)$ angle that deviates from 180°. For $Ta_2Ni_3S_8$ this angle is 162.0(2)° and for $Ta_2Pt_3Se_8$ it is 164.8(2)° in satisfactory agreement with the theoretical value 164° for the C_{4v}-square-pyramidal fragment ML_5 where M is a d^8 atom (*11*). The structural results for $Ta_2M_3Q_8$ (M = Ni, Pt) are consistent with the simple valence description Ta^{V}, M^{II}, Q^{-II}.

The temperature dependence of the single-crystal conductivity of $Ta_2Ni_3S_8$ in the region 100–300 K is illustrated in Fig. 2. The conductivity attains a maximum of 0.8 ohm^{-1} cm^{-1} at 207 K and then shows little change as the temperature is raised. This same behavior is observed for $Nb_2Pd_3Se_8$ (*1*) and is consistent with the presence of d^0 Ta^{V} and d^8 Ni^{II}.

$Ta_2Pd_{0.89}S_5$. This compound is isostructural with $Nb_2Pd_{0.71}Se_5$, which has been described in detail (*2*). The structure is shown

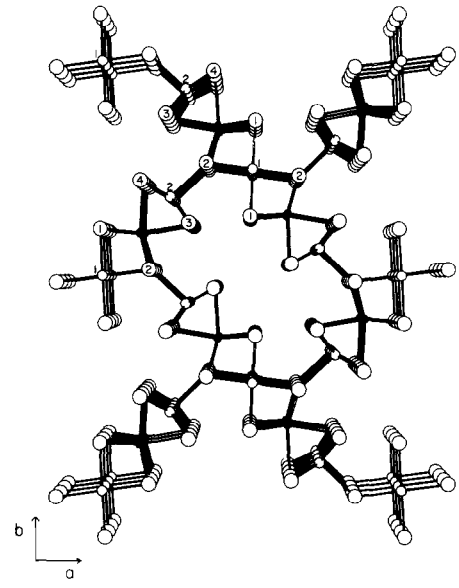

FIG. 1. Perspective view of the $Ta_2M_3Q_8$ structure down [001], showing the labeling scheme. Small filled circles are Ta atoms, small open circles are Ni or Pt atoms, and large open circles are S or Se atoms.

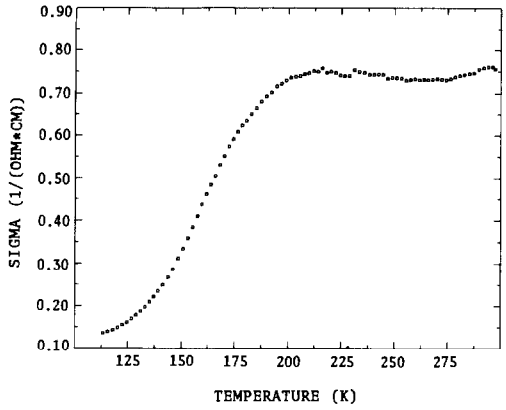

FIG. 2. Temperature dependence of the single-crystal conductivity along the needle axis c for $Ta_2Ni_3S_8$.

TABLE VI

SELECTED BOND DISTANCES (Å) AND ANGLES (DEG.) FOR $Ta_2Pd_{0.89}S_5$

Pd(1)–2S(3)	2.342(4)	S(3)–Pd(1)–S(4)	84.10(14)
Pd(1)–2S(4)	2.325(4)	S(1)–Pd(2)–S(1)	84.78(13)
Pd(1)–2Pd(1)	3.269(2)	S(2)–Ta(1)–S(3)	84.50(12)
Pd(2)–4S(1)	2.425(3)	S(2)–Ta(1)–S(5)	79.64(13)
Ta(1)–S(2)	2.458(4)	S(3)–Ta(1)–S(3)	83.30(13)
Ta(1)–2S(3)	2.460(3)	S(3)–Ta(1)–S(4)	79.03(11)
Ta(1)–2S(4)	2.453(3)	S(4)–Ta(1)–S(4)	83.58(13)
Ta(1)–S(5)	2.437(4)	S(4)–Ta(1)–S(5)	83.13(11)
Ta(1)–2Ta(1)	3.269(2)	S(1)–Ta(2)–S(1)	79.64(12)
Ta(2)–2S(1)	2.553(3)	S(1)–Ta(2)–S(2)	79.90(12)
Ta(2)–S(1)	2.645(4)	S(1)–Ta(2)–S(5)	73.09(11)
Ta(2)–2S(2)	2.465(3)	S(2)–Ta(2)–S(2)	83.09(12)
Ta(2)–2S(5)	2.475(3)	S(2)–Ta(2)–S(5)	78.78(11)
Ta(2)–2Ta(2)	3.269(2)	S(5)–Ta(2)–S(5)	82.67(13)

in Fig. 3. Selected bond distances and angles for $Ta_2Pd_{0.89}S_5$ are presented in Table VI. These are consistent with those found earlier in $Nb_2Pd_{0.71}Se_5$, when account is taken of the differing crystal radii of S and Se (*10*). The Pd–S and Ta–S distances are consistent with similar interactions in PdS (*12*) and TaS_3 (*13*).

The electrical conductivity of crystals of $Ta_2Pd_{0.89}S_5$ has been measured over the temperature range 110–285 K. These data, presented in Fig. 4, are consistent with the behavior expected for a metallic conductor. As the shortest S–S distance in this compound, S(1)–S(5) = 2.995(5) Å, is indicative of the absence of S–S interactions, we adopt the partial valence description Pd^{II}, S^{-II}. The Ta atoms then have a formal valence intermediate between V and IV, or alternatively, a band of primarily Ta d-character is partially filled, thus giving rise to the observed metallic properties.

$Co_2Nb_4PdSe_{12}$. This material (Figs. 5 and 6) is isostructural with $Co_2Ta_4PdSe_{12}$, which has been described in detail (*2*). The metrical data of Table VII reveal only very small

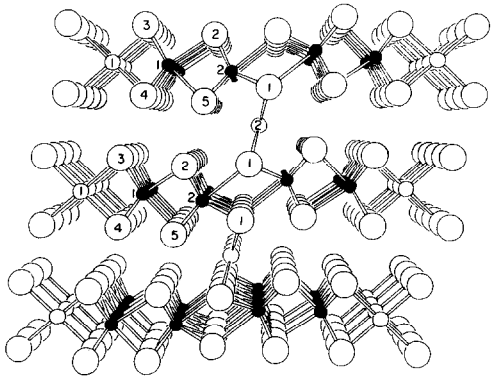

FIG. 3. Perspective view of the $Ta_2Pd_{0.89}S_5$ structure down [010], showing the labeling scheme. Ta atoms are small filled circles, Pd atoms are small open circles, and S atoms are large open circles. Site Pd(2) is 78.6(4)% occupied.

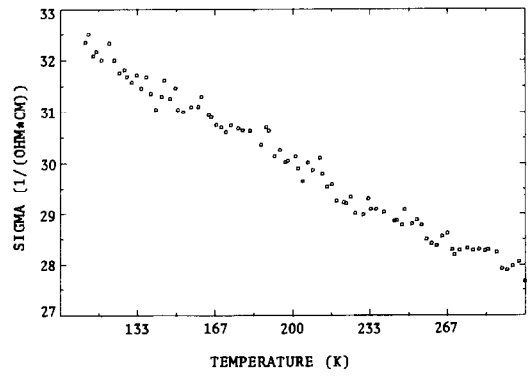

FIG. 4. Plot of conductivity vs temperature for single crystals of $Ta_2Pd_{0.89}S_5$, measured along the needle axis b.

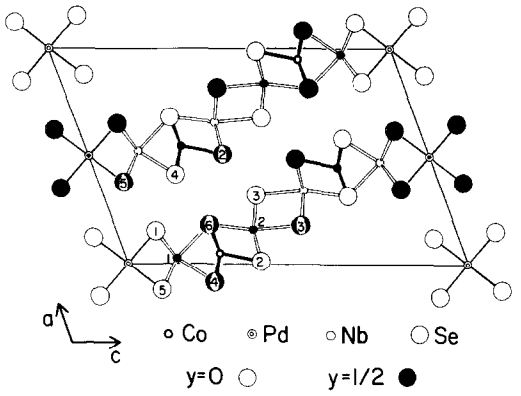

FIG. 5. Projection of the $Co_2Nb_4PdSe_{12}$ structure showing the labeling scheme.

differences from the Ta structure. Most notable are the lengthening of the Nb(2)–Se(6) bond and an opening of the apical Se(6)–Nb(2)–Se(3) bond angle.

Discussion

We have established through the synthesis and characterization of $Ta_2Ni_3S_8$ that Ni can be substituted for Pd in both the square-planar and square-pyramidal environments in the $Nb_2Pd_3Se_8$ structural type (*1*). That this can be accomplished is not too surprising, as Ni chalcogenides with Ni in square-planar (*6*) and square-pyramidal (*8*) sites are known. Yet the conditions for formation of $Ta_2Ni_3S_8$ are not very different from those for Ta_2NiS_5 (*4*) in which Ni occupies a tetrahedral site and Ta an octahedral site. Attempts to prepare the Pd analogue of Ta_2NiQ_5 have not been successful. Clearly Ni shows considerably more variability in its coordination geometry than does Pd.

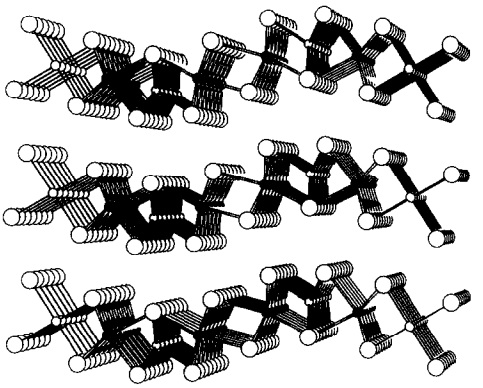

FIG. 6. Perspective view of the $Co_2Nb_4PdSe_{12}$ structure down [010]. Nb atoms are small filled circles, Pd atoms are small open circles with narrow bonds, Co atoms are small open circles with thick bonds, and Se atoms are large open circles. From left to right are chains of square-planar Pd atoms, trigonal-prismatic Nb atoms, square-pyramidal Co atoms, and octahedral Nb atoms.

We have established through the synthesis and characterization of $Ta_2Pt_3Se_8$ that Pt can also be substituted for Pd in the two environments in the $Nb_2Pd_3Se_8$ structural type. We have found that Pt is difficult to transport, and $Ta_2Pt_3Se_8$ is the first compound to contain Pt that we have made in the form of single crystals. Thus we have little knowledge of the stereochemical preferences of Pt in the ternary chalcogenides of interest here. We expected Pt to substitute for Pd in square-planar sites since binary and ternary chalcogenides with Pt in this environment are known (*14–16*). The presence of Pt in a square-pyramidal geom-

TABLE VII

SELECTED BOND DISTANCES (Å) AND ANGLES (DEG.) FOR $Co_2Nb_4PdSe_{12}$

Co–2Se(4)	2.379(2)	Se(2)–Co–Se(4)	88.99(9)
Co–2Se(6)	2.420(2)	Se(2)–Co–Se(6)	112.90(8)
Co–Se(2)	2.384(3)	Se(4)–Co–Se(4)	91.29(11)
Co–2Nb(2)	2.908(3)	Se(1)–Nb(1)–Se(1)	81.88(8)
Co–2Nb(1)	2.995(3)	Se(1)–Nb(1)–Se(5)	80.55(7)
Co–2Co	3.402(2)	Se(1)–Nb(1)–Se(6)	84.22(8)
Nb(1)–2Se(1)	2.596(2)	Se(4)–Nb(1)–Se(5)	83.90(8)
Nb(1)–Se(4)	2.524(3)	Se(4)–Nb(1)–Se(6)	78.14(9)
Nb(1)–2Se(5)	2.599(2)	Se(2)–Nb(2)–Se(2)	83.76(9)
Nb(1)–Se(6)	2.639(3)	Se(2)–Nb(2)–Se(3)	95.88(7)
Nb(1)–2Pd	3.267(2)	Se(2)–Nb(2)–Se(6)	103.16(7)
Nb(1)–2Nb(1)	3.402(2)	Se(3)–Nb(2)–Se(3)	81.79(9)
Nb(2)–2Se(2)	2.548(2)	Se(3)–Nb(2)–Se(6)	89.05(7)
Nb(2)–2Se(3)	2.598(2)	Se(6)–Nb(2)–Se(3)	172.02(8)
Nb(2)–Se(3)	2.686(3)	Se(1)–Pd–Se(5)	86.89(8)
Nb(2)–Se(6)	2.562(3)		
Nb(2)–2Nb(2)	3.402(2)		
Pd–2Se(1)	2.435(2)		
Pd–2Se(5)	2.448(2)		
Pd–2Pd	3.402(2)		

etry is more surprising as, to our knowledge, this is the first time that this coordination about Pt has been clearly established in an inorganic solid-state chalcogenide.

Although the substitution of Ta for Nb in the trigonal-prismatic and monocapped trigonal-prismatic sites of $Nb_2Pd_{0.71}Se_5$ is not surprising, an interesting difference between $Nd_2Pd_{0.71}Se_5$ and $Ta_2Pd_{0.89}S_5$ is in the occupancy of the square-planar Pd(2) site in the van der Waals' gap (41.9(5)%, Nb compound; 78.6(4)%, Ta compound). This result demonstrates the stoichiometric variability of this site, a site that involves only coordination by the $Q(1)$ atoms. Thus it should be possible to modify the physical properties of these phases by change in the occupancy of this site with minimum disruption of the rest of the structure.

The $Co_2Ta_4PdSe_{12}$ structural type contains Ta in both trigonal-prismatic and octahedral sites. It is known that these two coordination geometries for Ta are of very similar stability (*17–19*). But the situation is different for Nb. Although octahedral coordination for Nb is common in halides (*20*), oxides (*21*), and numerous molecular species (*22*), it is distinctly rarer in pure chalcogenides. Among the few known examples are the high-temperature forms of the layered compounds $NbSe_2$ (*23*) and $NbTe_2$ (*24*) and the series of compounds with the Nb_3FeSe_{10} structure (*25, 26*), in which one of the crystallographically independent Nb atoms is disordered with Fe over an octahedral site. Thus the successful synthesis of $Co_2Nb_4PdSe_{12}$, in which Nb has been substituted for Ta in both the trigonal-prismatic and octahedral sites of the $Co_2Ta_4PdSe_{12}$ structural type (*2*), is of particular interest. This unexpected result suggests that in some instances the basic stability of a structural type can force a given metal atom into a less-favored coordination geometry. Nevertheless the concept of stereochemical preferences of metal atoms as applied to the design of new solid-state materials remains a useful alternative to the more usual description of cations filling anion interstices.

Acknowledgments

This work was supported by the U.S. National Science Foundation—Solid State Chemistry—Grant DMR-83-15554. Some of the measurements were carried out in the SEM and X-ray Facilities of Northwestern University's Material Research Center, supported in part under the NSF-MRL program (Grant DMR82-16972).

References

1. D. A. KESZLER AND J. A. IBERS, *J. Solid State Chem.* **52,** 73 (1984).
2. D. A. KESZLER, J. A. IBERS, M. SHANG, AND J. LU, *J. Solid State Chem.* **57,** 68 (1985).
3. D. A. KESZLER, P. J. SQUATTRITO, N. E. BRESE, J. A. IBERS, M. SHANG, AND J. LU, *Inorg. Chem.* **24,** 3063 (1985).
4. S. A. SUNSHINE AND J. A. IBERS, *Inorg. Chem.* **24,** 3611 (1985).
5. D. A. KESZLER AND J. A. IBERS, *J. Amer. Chem. Soc.* **107,** 8119 (1985).
6. W. BRONGER, J. EYCK, W. RÜDORFF, AND A. STÖSSEL, *Z. Anorg. Allg. Chem.*, **375,** 1 (1970).
7. O. KNOP, K. I. G. REID, SUTARNO, AND Y. NAKAGAWA, *Canad. J. Chem.* **46,** 3463 (1968).
8. G. ÅKESSSON AND E. RØST, *Acta Chem. Scand. Ser. A* **29,** 236 (1975).
9. T. E. PHILLIPS, R. P. SCARINGE, B. M. HOFFMAN, AND J. A. IBERS, *J. Amer. Chem. Soc.* **102,** 3435 (1980).
10. R. D. SHANNON, *in* "Structure and Bonding in Crystals" (M. O'Keeffe and A. Navrotsky, Eds.), Vol. 2, p. 53, Academic Press, New York (1981).
11. A. R. ROSSI AND R. HOFFMANN, *Inorg. Chem.* **14,** 365 (1975).
12. N. E. BRESE, P. J. SQUATTRITO, AND J. A. IBERS, *Acta Crystallogr.* **C41,** 1829 (1985).
13. A. MEERSCHAUT, L. GUEMAS, AND J. ROUXEL, *J. Solid State Chem.* **36,** 118 (1981).
14. O. GÜNTHER AND W. BRONGER, *J. Less-Common Met.* **31,** 255 (1973).
15. W. BRONGER, O. GÜNTHER, J. HÜSTER, AND M. SPANGENBERG, *J. Less-Common Met.* **50,** 49 (1976).
16. F. GRØNVOLD, H. HARALDSEN, AND A. KJEKSHUS, *Acta Chem. Scand.* **14,** 1879 (1960).
17. R. HUISMAN, R. DE JONGE, C. HAAS, AND F. JELLINEK, *J. Solid State Chem.* **3,** 56 (1971).
18. F. R. GAMBLE, *J. Solid State Chem.* **9,** 358 (1974).

19. M. KERTESZ AND R. HOFFMANN, *J. Amer. Chem. Soc.* **106,** 3453 (1984).
20. A. ZALKIN AND D. E. SANDS, *Acta Crystallogr.* **11,** 615 (1958).
21. L. KATZ AND H. MEGAW, *Acta Crystallogr.* **22,** 639 (1967).
22. F. COTTON AND G. WILKINSON, "Advanced Inorganic Chemistry," 4th ed., pp. 831–844, Interscience, New York (1980), and references therein.
23. F. KADIJK AND F. JELLINEK, *J. Less-Common Met.* **23,** 437 (1971).
24. J. VAN LANDUYT, G. VAN TENDELOO, AND S. AMELINCKX, *Acta Crystallogr. Sect. A* **31,** S85 (1975).
25. A. MEERSCHAUT, P. GRESSIER, L. GUEMAS, AND J. ROUXEL, *Mater. Res. Bull.* **16,** 1035 (1981).
26. A. BEN SALEM, A. MEERSCHAUT, L. GUEMAS, AND J. ROUXEL, *Mater. Res. Bull.* **17,** 1071 (1982).